[Papers in Palaeontology, 2023, e1482]

Phylogenetic position of *Bohemiacinctus* gen. nov. (Echinodermata, Cincta) from the Cambrian of Bohemia: implications for macroevolution and the role of taxon sampling in palaeobiological systematics

by SAMUEL ZAMORA[1,2,*], DAVID F. WRIGHT[3,4,5,*] *and* MARTINA NOHEJLOVÁ[6]

[1]Instituto Geológico y Minero de España (IGME-CSIC), 50006 Zaragoza, Spain; s.zamora@igme.es
[2]Grupo Aragosaurus-IUCA, Área de Paleontología, Facultad de Ciencias, Universidad de Zaragoza, Zaragoza, Spain
[3]Sam Noble Museum, 2401 Chautauqua Ave, Norman, Oklahoma 73072, USA; wrightdf@ou.edu
[4]School of Geosciences, University of Oklahoma, 100 E. Boyd St, Norman, Oklahoma 73019, USA
[5]Department of Paleobiology, National Museum of Natural History, Smithsonian Institution, Washington, District of Columbia 20560, USA
[6]Czech Geological Survey, Prague 11821, Czech Republic; martina.nohejlova@geology.cz
*Corresponding author

Typescript received 21 April 2022; accepted in revised form 27 October 2022

Abstract: '*Asturicystis*' *havliceki* Fatka & Kordule from the middle Cambrian of Bohemia (Czech Republic) is re-described based on its type material. Several features, including the extension of the food grooves and presence of ventral swellings suggest that '*A.*' *havliceki* does not belong to *Asturicystis*, and is placed in the new genus *Bohemiacinctus*. To ascertain the phylogenetic position of *Bohemiacinctus havliceki*, we conducted Bayesian fossil tip-dating and parsimony-based phylogenetic analyses of 24 species spanning all major groups of cinctan higher taxa. Results show a high degree of congruence between tree topologies recovered by both tip-dated and parsimony-based analyses. Both methods indicate *B. havliceki* is phylogenetically distant from *Asturicystis* and is most likely to be an early representative of the family Sucocystidae. Overall, our phylogeny is broadly similar to previous estimates of cinctan relationships, including a more conventional phylogenetic position of controversial taxa such as *Protocinctus*. These results point to the sensitivity of small clades such as cinctans to taxon sampling effects, and highlights the importance of taxonomy and accurate morphological character descriptions in phylogenetic analyses of fossil taxa.

Key words: echinoderm, Gondwana, phylogeny, *Asturicystis*, Sucocystidae.

CINCTANS include a small group of echinoderms restricted to the Miaolingian of Gondwana (including Avalonia) and Siberia (Friedrich 1993; Rozhnov 2006; Zamora *et al.* 2013*a*). They are bizarre echinoderms with an almost symmetric body displaying a characteristic racket-like shape (Ubaghs 1967). Despite this trend to a general bilateral shape, cinctans have an asymmetric main feeding structure. The mouth of cinctans lies in the anterior right side of the marginal frame (cinctus), where one or more, generally two, asymmetric food grooves converge (Ubaghs 1975), and which has been considered one of the main characteristics of the group (Barrande 1887; Jaekel 1918). Anteriorly, cinctans possessed a large diagnostic plate called the operculum, which covered the porta (an anterior central opening) in life (Sdzuy 1993).

Despite important advances in the systematics (Zamora & Smith 2008; Zamora *et al.* 2013*b*), distribution (Zamora & Álvaro 2010), phylogeny (Smith & Zamora 2009; Wright *et al.* 2021) and palaeobiology (Rahman *et al.* 2015, 2020) of cinctans, there are still gaps in the knowledge of the group. For example, some species are still poorly documented and there are many others that need further description in order to clarify in-group phylogenetic relationships (Smith & Zamora 2009).

One such poorly described species is '*Asturicystis*' *havliceki* Fatka & Kordule, 2001. This species was the third cinctan species described from Bohemia (Czech Republic) and was originally represented by a few specimens of dorsal and ventral views of the theca (Fatka & Kordule 2001). The age of '*A.*' *havliceki* is middle–late Leonian according to regional stage (*sensu* Sdzuy *et al.* 1999), which corresponds to the global Wuliuan Stage of the Miaolingian, and is approximately equivalent to the occurrence of *Protocinctus mansillaensis*, the oldest species of cinctan

doi: 10.1002/spp2.1482

described from Spain (Rahman & Zamora 2009). Thus, it is one of the oldest reported cinctans but its morphology requires re-examination (Smith & Zamora 2009).

The aims of this paper are first to re-evaluate to taxonomic status of '*A*.' *havliceki* and more completely redescribe its morphology; second, to codify the morphological features of this important species and append it to a pre-existing character matrix of cinctan taxa to ascertain its phylogenetic position; and finally, to evaluate the current status of alternative hypotheses regarding cinctan phylogeny and evolution.

MATERIAL AND METHOD

Material

Specimens described in this paper are the same as those originally reported by Fatka & Kordule (2001). They include six specimens deposited in the Czech Geological Survey of Prague under the acronyms VK1, VK2, VK3, VK4, VK5 and VK6 (Fig. 1). Three specimens (VK1, VK2 and VK6) preserve both the upper and lower surfaces; VK3 is represented by a lower surface (Fig. 1I), the anterior part of which clearly shows the extension of the food grooves; VK4 is represented by half of the anterior part of a theca in ventral view, which shows details of the left food groove, the closed operculum and right adopercular process (Fig. 1G, H); and VK5 is represented by a complete upper theca preserving the stele (Fig. 1A). Contrary to what was previously indicated by Fatka & Kordule (2001), most anatomical information from '*A*.' *havliceki* is available in this collection. A seventh specimen (VK7) was considered by Fatka & Kordule (2001) as '*A*'. cf. *havliceki* (Fig. 1D) because of 'its lower number of marginal (M4l-M5r)' and then doubtfully assigned to the same species, a view that we follow here. Despite the number of marginal plates, '*A*'. cf. *havliceki* also has a left food groove extending one plate less (M1l) than in '*A*.' *havliceki*. This is interesting because in all other features this specimen is identical to the rest. Thus, it may be possible that the one missing plate in the anterior part is the reason for the differences in morphology.

Specimens were cast using latex and then photographed covered with sublimated ammonium chloride.

Phylogenetic analysis

Character data for phylogenetic analyses come from a pre-existing character matrix initially published by Smith & Zamora (2009) and subsequently augmented by Zamora *et al.* (2013*b*). These studies were the first to use maximum parsimony-based phylogenetic analysis to evaluate evolutionary relationships within the class Cincta. Recently, Wright *et al.* (2021) reanalysed the character matrix of Zamora *et al.* (2013*b*) to infer patterns of morphological disparity, speciation mode and phylogenetic relationships using Bayesian tip-dating methods (Gavryushkina *et al.* 2017; Wright 2017; Warnock & Wright 2020). In this study we use our redescription of '*A*.' *havliceki* to code and append this important species into the character matrix previously analysed by Zamora *et al.* (2013*b*) and Wright *et al.* (2021) (Appendix). In total, our new matrix comprises 23 cinctan species and 60 morphological characters, with *Ctenocystis utahensis* included to provide outgroup polarization and root the parsimony trees. To facilitate comparison across studies, we conducted a phylogenetic analysis of the updated character matrix using both Bayesian fossil tip-dating methods and parsimony analysis.

Maximum parsimony analysis was conducted using PAUP* (Swofford 2002) via a heuristic search using 1000 random addition sequence replicates. Branch swapping was performed using tree bisection reconnection. All characters were treated as unordered and equally weighted. Results were summarized by calculating the tree length (i.e. number of parsimony steps), consistency index (CI) and the retention index (RI) for the most parsimonious trees (MPTs) recovered in the analysis, and computing the strict consensus and 50% majority rule topologies.

Bayesian tip-dating analysis was conducted using the fossilized birth–death process (FBD) (Stadler 2010; Heath *et al.* 2014; Wright 2017; Gavryushkina *et al.* 2017; Stadler *et al.* 2018). In their reanalysis of the matrix of Zamora *et al.* (2013*b*), Wright *et al.* (2021) fitted a variety of complex, hierarchical Bayesian models that varied in assumptions regarding how morphological characters evolve, how evolutionary rates vary across the tree, and whether rate shifts are coincident with geologic intervals. Wright *et al.* (2021) used stepping-stone analysis

FIG. 1. *Bohemiacinctus havliceki* (Fatka & Kordule) (A–C, E–I) and *B.* cf. *havliceki* (D) from the middle Cambrian of Bohemia (Barrandian area, Czech Republic). A, dorsal view of the holotype (VK5) showing 11 marginal plates. B, C, E, dorsal (B), ventral (C) and frontal (E) views of specimen VK6, showing the porta-operculum complex, distribution of ventral swellings and food grooves in the anterior part; arrows (E) indicate the extent of the food grooves. D, *Bohemiacinctus* cf. *havliceki* (VK7) showing an extra plate in the cinctus. F, I, frontal and ventral view of VK3 showing the distribution of food grooves and ventral swellings; arrows (F) indicate the extent of the food grooves. G–H, ventral and frontal views of specimen VK4. All specimens are latex casts whitened with sublimated ammonium chloride. *Abbreviations*: M, marginal plate; Op, operculum; Pe, peristome; Rap, right adopercular process. All scale bars represent 2 mm.

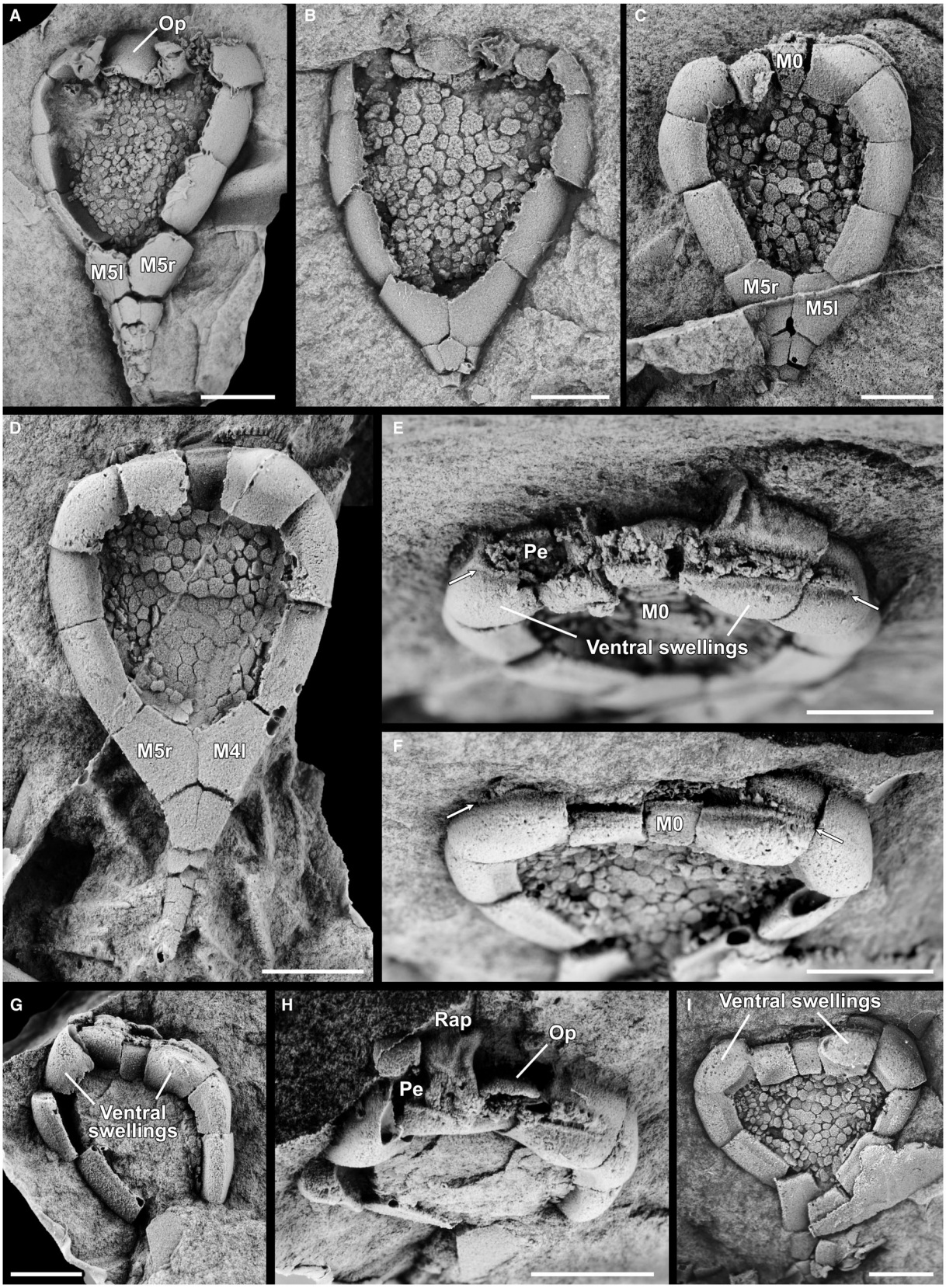

(Xie *et al.* 2011) to estimate marginal likelihoods for each model to determine the best-fit model using Bayes factors (Kass & Raftery 1995). Rather than reproduce this computationally intensive procedure, we apply the same best-fit model configuration as determined by Wright *et al.* (2021) to our updated character matrix. In brief, morphological evolution is modelled using Lewis' (2001) Mk equations with rate variation following a lognormal distribution (Wagner 2012). To account for rate variation across different branches in the tree, we also used an uncorrelated lognormal distribution (Drummond *et al.* 2006). Tip-ages were sampled from uniform prior distributions based on their first and last appearances, and separate FBD parameters were estimated for each geologic stage. See Wright *et al.* (2021) for additional details regarding model configuration and implementation.

A posterior distribution of phylogenies was estimated using Markov-chain Monte Carlo (MCMC) analysis in the phylogenetic software *RevBayes* (Höhna *et al.* 2016). Based on convergence diagnostics in Wright *et al.* (2021), we ran MCMC for 70 000 generations (sampling every 10 steps) following an initial burn-in interval of 15 000 generations tuning parameters every 200 steps. Convergence was assessed using the software Tracer (Rambaut *et al.* 2018). The maximum clade credibility tree was selected as a Bayesian point estimate of cinctan phylogeny, with clade posterior probabilities at each node informed by the entire posterior distribution of trees.

RESULTS

The results of both phylogenetic analyses are jointly summarized in Figure 2. Maximum parsimony analysis resulted in 27 MPTs, each with a tree length of 177 steps, CI = 0.554, and RI = 0.646. The Bayesian tip-dating analysis resulted in a posterior distribution of 7000 trees. Overall, our results are broadly similar to phylogenies recovered in previous studies and exhibit a close but imperfect correspondence between family-level classification and cinctan phylogeny (Fig. 2). For example, all members of the Gyrocystidae are recovered as forming a monophyletic group except for *Graciacystis ambigua*, which is sister to *Sotocinctus ubaghsi* (previously considered a trochocystitidid) in both maximum parsimony and Bayesian analyses (Fig. 2). Similarly, both analyses recover two trochocystitidid species, *Trochocystites bohemicus* and *Trochocystoides parvus*, as reciprocally monophyletic. Aside from controversial taxa such as *Protocinctus*, both analyses support the monophyly of the Family Sucocystidae, which is recovered as sister to the trochocystitidid clade (posterior probability = 0.56, 100% MPTs). In both maximum parsimony and Bayesian tip-dating analyses, the phylogenetic position of '*A.*' *havliceki* is strongly supported within the Sucocystidae + (*Trochocystites* + *Trochocystoides*) clade and is recovered in our phylogeny as an early representative of the Sucocystidae. '*Asturicystis*' *havliceki* is therefore a plesiomorphic species within the Sucocystidae, in a distinct clade and phylogenetically distant from *Asturicystis jaekeli*, from which it differs in a number of important features (see below). Thus, a new genus *Bohemiacinctus* is erected to accommodate *B. havliceki* (Fatka & Kordule, 2001).

Institutional abbreviation. Specimens are deposited in the Czech Geological Survey of Prague under the acronym VK.

SYSTEMATIC PALAEONTOLOGY

Nomenclature and orientation follow Friedrich (1993); this is the optimal scheme for recognizing homologies among cinctan taxa (Smith & Zamora 2009). The marginal plate that coincides with the axial plane is named M0, and the remainder of the marginal plates are numbered as M1r–M5r or M1l–M5l, depending on whether their position is right (r) or left (l) of M0 (in plan view).

Phylum ECHINODERMATA Bruguière, 1791 *ex* Klein, 1734
Class CINCTA Jaekel, 1918
Family SUCOCYSTIDAE Friedrich, 1993
Genus BOHEMIACINCTUS nov.

LSID. https://zoobank.org/nomenclaturalacts/747FFA18-9030-418F-9993-10EF37C9D02A

Type and only species. Bohemiacinctus havliceki new. comb.

Derivation of the name. Named after Bohemia, the region where type material was originally described.

Diagnosis. Sucocystidae with 11 marginal plates in the cinctus (M5r–M5l). Two marginal grooves, right one extending up to M2r and left up to M2l. Well-developed swellings as two large continuous structures that run from half of M1l to the end of M3l and from M1r to the end of M4r, and anteriorly interrupted along M0. Poorly developed adopercular processes and poorly differentiated lintel composed of four supracentral plates.

Remarks. Bohemiacinctus havliceki displays a combination of characters that are unique, rather than clear autapomorphies. The length of the left food groove is shared with *Asturicystis jaekeli* and *Sotocinctus ubaghsi*, but the right one is shorter, and similar to *Undatacinctus*, *Lignanicystis* and *Elliptocinctus*. Moreover, it has clear ventral swellings

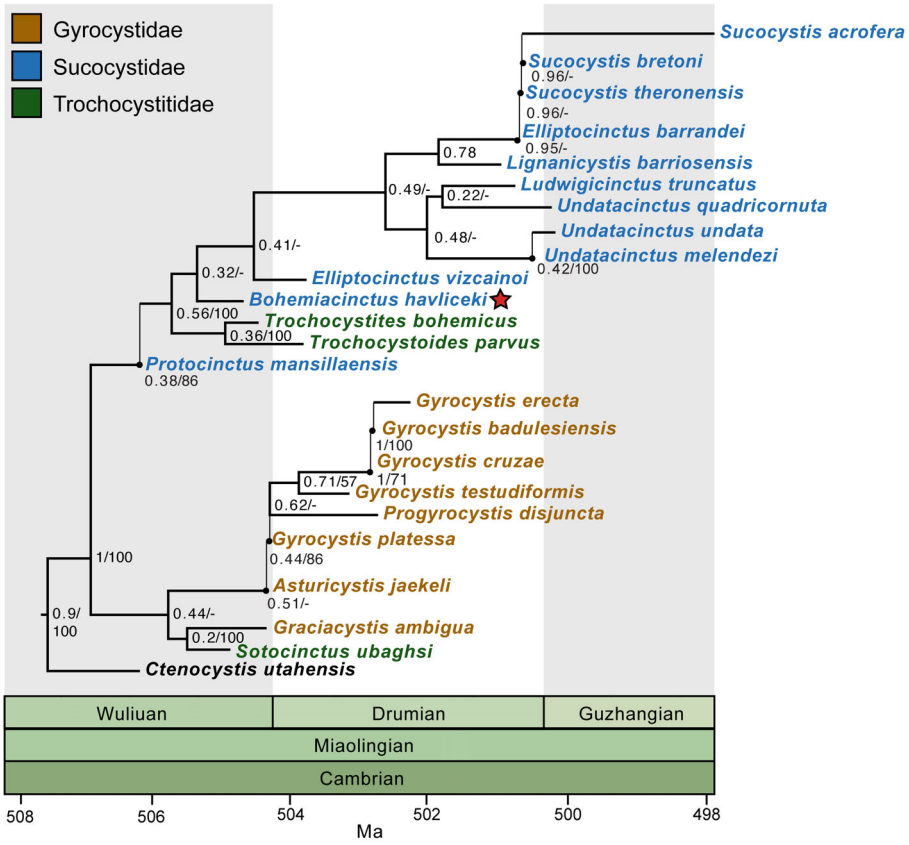

FIG. 2. Results from Bayesian tip-dating and maximum parsimony analyses of phylogeny. The phylogeny shown is the maximum clade credibility (MCC) tree from the posterior distribution. Values at the nodes indicate clade support as posterior probabilities (left) and the degree of congruence between the MCC tree and results from parsimony analysis (right), where congruence is measured as the frequency of clades in the most parsimonious trees shared with the MCC tree. Vertical branches without splits indicate ancestor–descendant relationships in the form of either anagenesis or 'budding' speciation. Although stratigraphic ranges were used for tip-dated tree inference, the tip ages shown here represent point occurrences sampled in the MCC tree and thus do not reflect the full stratigraphic age or divergence time distributions. The star indicates the position of *Asturicystis havliceki* Fatka & Kordule, reinterpreted herein as *Bohemiacinctus havliceki*.

that are absent in plesiomorphic forms such as *Sotocinctus* and *Asturicystis*, but common in derived Sucocystidae.

Bohemiacinctus havliceki comb. nov.
Figures 1, 3

2001 *Asturicystis havliceki*; Fatka & Kordule, figs 1, 2

LSID. https://zoobank.org/nomenclaturalacts/D4E2D24E-F3FD-4149-AAE7-B75BEF6CF3F8

Type specimens. Holotype VK5 is a dorsal surface preserving the stele (Fig. 1A). Paratypes include specimens VK1–VK4, VK6.

Diagnosis. As for the monotypic genus.

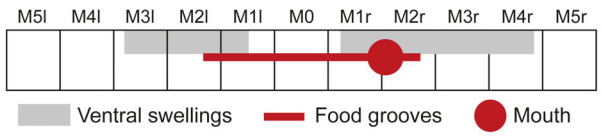

FIG. 3. Schematic plate diagram of *Bohemiacinctus havliceki* indicating the extent of the food grooves, the plates from the cinctus and the development of ventral swellings. See Smith & Zamora (2009) for comparison with other cinctan species.

Description

The theca consists of 11 marginal plates (M5r–M5l) and several hundred integument plates. It ranges in size from approximately 6–7 mm in length and 5–6 mm in width; the thecal outline is subtriangular. The stele measures at least 2 mm in length, but it is incomplete.

Orifices. Only two openings are preserved in the theca of *Bohemiacinctus*, which correspond to the porta and the peristome. The porta lies at the anterior extremity of the theca, passing through the marginal frame coincident with the axial plane and is framed by M1r, M1l and underlain by M0. In all specimens it is covered by the operculum. The upper margin of the opening is bordered by four plates of the supracentral integument (the lintel) (Fig. 1B). The operculum is approximately 1 mm in length in the axial direction and 1.5 mm in width, and it completely filled the porta during life (Fig. 1A, H). It is smooth on its inner concave face but slightly ornamented on its external, convex face.

The second preserved aperture (peristome) is a small circular aperture that passes through the anterior right side of the cinctus between marginal plates M1r and M2r and is covered dorsally by the supraoral plate (Fig. 1E). The opening is slightly flattened dorsoventrally and is wider than tall in external view. On the interior, M1r and M2r form a broad, expanded platform ventral to the opening. Externally, two marginal grooves lead from the left and the right into this aperture.

Cinctus. The cinctus is composed of 11 marginal plates that vary in size and shape around the ring (Fig. 1A–C). All are approximately triangular in cross-section, with short, thick, concave internal faces and wide, wedge-shaped outer faces.

M0 is a subrectangular plate located at the anterior extremity of the cinctus that forms the floor of the porta. It is flat on its ventral surface, slightly wider anteriorly than posteriorly in plan view and bears a single marginal groove on its outer face. There is no broad anterior shelf to this plate; the marginal groove runs beneath the ambitus and faces forwards.

M1r and M1l form the lateral frame to the porta, each giving rise to a small dorsal adopercular process. Both plates are subrectangular in ventral view and are in contact with the supracentral and infracentral integument. M1r also is in contact with the supraoral plate, M0 and M2r; M1l is in contact with M0 and M2l. The suropercular facets are not observable in the available specimens. The adopercular processes are poorly preserved but inclined slightly towards the anterior. M1r and M1l carry portions of the marginal groove on their outer surfaces. M2r is sub-trapezoidal. M3r is very similar to the other mid-cinctus plates, having a swelling ventral surface with a rectangular outline and lacking an outer flange on its dorsal surface. M4r is longer than M3r. Its posterior margin is in contact with M5r, which articulates with the stele.

The left marginal plates of the cinctus (M2l, M3l, M4l) are similar to those of other cinctan species. M5l forms the articulation with the stele and closes the cinctus in contact with M5r. Swellings are distributed as two large continuous structures that run from half of M1l to the posterior extremity of M3l and from M1r to the end of M4r. These structures are interrupted in M0.

Integuments. The supracentral (dorsal) and infracentral (ventral) integuments are composed of a large number of small polygonal plates. They have a similar size in both integuments, but in some specimens they seem to be slightly smaller in the dorsal integument than in the ventral.

The plates making up the supracentral integument (Fig. 1B) are ornamented externally with small crests and slightly decrease in size posteriorly. The infracentral integument (Fig. 1C, I) is composed of polygonal tessellate plates that also appear to be slightly ornamented. The sutures of supracentral plates bear an invagination for the attachment of ligaments, while infracentral plates have flatter sutures.

Marginal groove. Marginal grooves run left and right from the mouth around the outer face of the marginal ring to M2l and M2r, respectively (Fig. 1E–G). At the anterior extremity of the theca, the left groove lies below the ambitus, and thus faces frontally. A weakly developed rim borders the marginal groove at the articulation of the labrum plates. Some specimens preserve part of the labrum (Fig. 1C, D), which is composed of a sheet of small platelets, with at least one sheet of plates that articulate to the cinctus on each side covered with another set of cover plates each.

Stele. The stele originates as a direct continuation of the marginal frame (Fig. 1A). It is approximately half longer than the theca. It is constructed from a marginal series of wedge-shaped sphenoid plates, with smaller polygonal mesosphenoidal plates along the dorsal midline. Mesosphenoid plates along the dorsal part of the stele are uniserially arranged. In cross-section the stele is rounded on its dorsal surface but flat on its ventral part.

Remarks

Many of the features described in the present study were misinterpreted in the original description of '*A.*' *havliceki*, resulting in an incorrect genus-level placement. Smith & Zamora (2009) indicated that '*A.*' *havliceki* is unlikely to be a true *Asturicystis* because its food groove pattern is very different, and has ventral swellings. They also noted that it is probably a member of the Sucocystidae. Unfortunately, type material was not available for re-study at that time and these observations were not confirmed until now. *Bohemiacinctus havliceki* is different from *Asturicystis*

jaekeli in important features such as the extension of the food grooves that reach M2r and M2l in the former and M4r and M2l in the latter (Fig. 3). *Asturicystis jaekeli* also has a flat ventral surface lacking swellings, whereas they are present in *B. havliceki*. The presence of a right food groove extending to M2r is a feature shared between *B. havliceki* and some Sucocystidae such as *Elliptocinctus barrandei* and species of *Undatacinctus*. Many Sucocystidae also have large swellings on lateral parts of the cinctus. In contrast, *B. havliceki* lacks a ventral swelling on M0 and has a lintel that is poorly differentiated from other supracentral plates. All of these features suggest that this is a primitive member of Sucocystidae (see the phylogenetic discussion below).

Occurrence. Rejkovice 'Potůček', the Jince Formation, *Paradoxides* (*Eccaparadoxides*) *pusillus* Biozone, Příbram-Jince Basin, Barrandian area, Czech Republic. This corresponds with the Wuliuan, Miaolingian.

DISCUSSION

According to a previously published morphologic description and its taxonomic status, '*Asturicystis*' *havliceki* would be predicted to be sister to (or a close relative of) *Asturicystis jaekeli* (Fatka & Kordule 2001). However, based on our morphological redescription and taxonomic revision based on type material, we find that *Bohemiacinctus havliceki* is phylogenetically distant from *Asturicystis jaekeli* and instead recover *B. havliceki* as an early representative (both phylogenetically and temporally) of the Sucocystidae. With the inclusion of this important species, our revised phylogeny of cinctan taxa has several important implications for the understanding of their macroevolutionary patterns, as well as highlighting the sensitivity of phylogenetic inferences of fossil taxa to taxon sampling.

Phylogenetic trees of fossil taxa are increasingly being used to directly study macroevolutionary patterns and processes (Bapst 2014; Soul & Friedman 2015; Soul & Wright 2021; Černý *et al.* 2022). Similar to previous findings (Wright *et al.* 2021), our tip-dated analyses also recover evidence for ancestor–descendant relationships among members of the Gyrocystidae and Sucocystidae, which can arise either by speciation via 'budding' cladogenesis or anagenetic change within a morphospecies lineage (Eldredge 1971; Thuy *et al.* 2022). For example, instances of ancestor–descendant relationships in which the implied ancestor was still extant when the descendant lineage first appears provides evidence for 'budding' cladogenesis. Species pairs consistent with budding cladogenesis include the gyrocystids *Gyrocystis cruzae* and *G. badulesiensis*, as well as the sucocystids *Undatacinctus melendezi* and *U. undata*. Recovering evidence for such fine-scale macroevolutionary patterns, even in fossil taxa as geologically ancient and unassuming as cinctans, has major implications for the documentation of the tempo and mode of speciation in other fossil clades and time intervals.

Although our results are broadly similar to previous phylogenies for cinctan taxa (Zamora *et al.* 2013*b*; Wright *et al.* 2021), several clades differ with respect to the branching order of their ingroup species. In some cases, these differences have implications for the understanding of the patterns of character evolution. For example, *Protocinctus mansillaensis* is an important species for understanding the evolution of the water vascular system and feeding ecology in cinctans and is the oldest known representative of the clade (Rahman & Zamora 2009; Rahman *et al.* 2015). Previous studies placed *Protocinctus mansillaensis* as a basal member of the Sucocystidae, thereby supporting a phylogenetically derived position (Smith & Zamora 2009; Zamora *et al.* 2013*b*). In contrast, the Bayesian tip-dating analysis in Wright *et al.* (2021) recovered *P. mansillaensis* as sister to the entire cinctan clade. In our re-analysis, *P. mansillaensis* is placed as sister to the (*Trochocystites* + *Trochocystoides*) + *Sucocystidae* clade. Although the placement of *P. mansillaensis* in our phylogeny has low to modest support (posterior probability = 0.38, 86% MPTs), it is more similar to earlier interpretations of its phylogenetic position and implications for cinctan evolution (Rahman & Zamora 2009; Rahman *et al.* 2015).

Given that the broader aspects of cinctan phylogeny have remained stable since formal phylogenetic analysis began (Smith & Zamora 2009; Zamora *et al.* 2013*b*; Wright *et al.* 2021), what factors might influence the labile position of taxa such as *Protocinctus*? Simulations evaluating the efficacy of alternative phylogenetic methods indicate that Bayesian methods often outperform maximum parsimony (Wright & Hillis 2014), and tip-dated Bayesian methods often outperform undated analyses (Barido-Sottani *et al.* 2020; Mongiardino Koch *et al.* 2021). However, our results indicate substantial similarity in tree topologies recovered using both Bayesian tip-dating and maximum parsimony methods (Fig. 2), which effectively rules out the possibility that methodological differences produced the conflicting results. The difference in topologies between our new phylogeny and previous studies, therefore, may reflect the inclusion of *B. havliceki* in the present analysis. Taxon sampling is well known to affect all phylogenetic methods, including the accuracy of tree topologies, divergence times and diversification rates (Heath *et al.* 2008). Although the fossil record will always be incomplete, increasing taxon and character sampling can greatly increase the fidelity of phylogenetic methods for fossil taxa (Wagner 2000; Barido-Sottani *et al.* 2020; Mongiardino Koch *et al.* 2021). To the extent that phylogenetic and macroevolutionary inferences are affected by

incomplete or biased taxon sampling, it is important for palaeobiologists to sample as many taxa and characters as possible in their analyses.

CONCLUSION

'*Asturicystis*' *havliceki*, the oldest cinctan from Bohemia, is redescribed and included in the new genus *Bohemiacinctus*. A phylogenetic analysis is performed in order to understand its phylogenetic position. This places *Bohemiacinctus* as a plesiomorphic Sucocystidae and improves our understanding of this important clade of cinctans. The revision presented herein is significant not only for understanding phylogenetic relationships between cinctans, but it also highlights the important role of detailed taxonomic research and morphological investigations in the fields of phylogenetics, palaeobiology and macroevolution.

Acknowledgements. We appreciate comments from three referees, Bertrand Lefebvre, Brad Deline and Jeff Thompson, which greatly improved the resulting manuscript. We also appreciate the help and comments from the technical editor, Sally Thomas, and the editor, Imran A. Rahman. SZ was supported by the Spanish Ministry of Science, Innovation and Universities (PID2021-125585NB-I00), co-financed by the European Regional Development Fund, the project 'Aragosaurus: Recursos Geológicos y Paleoambientales' (E18_17R) funded by the Government of Aragon, and the grant AECEX2021 'Severo Ochoa extraordinary grants for excellence IGME-CSIC'. DFW was supported by the Smithsonian Institution. MN was supported by an internal grant from the Czech Geological Survey no. 310580, which is a contribution to the Strategic Research Plan of the Czech Geological Survey (DKRVO/ČGS 2018-2022).

Author contributions. **Conceptualization** S Zamora (SZ), DF Wright (DFW); **Investigation** SZ, DFW; **Methodology** SZ, DFW, M Nohejlová (MN); **Visualization** SZ, DFW, MN; **Writing – Original Draft Preparation** SZ, DFW; **Writing – Review & Editing** SZ, DFW, MN.

DATA ARCHIVING STATEMENT

This published work and the nomenclatural acts it contains, have been registered in ZooBank: https://zoobank.org/References/B29F9D09-6476-4994-B5AB-B26EEFAE7B2F

Data for this study are available in MorphoBank: http://morphobank.org/permalink/?P4328

All nexus-formatted data, scripts, and other supplemental files are available in Zenodo: http://doi.org/10.5281/zenodo.6863820

Editor. Imran Rahman

REFERENCES

BAPST, D. W. 2014. Assessing the effect of time-scaling methods on phylogeny-based analyses in the fossil record. *Paleobiology*, **40**, 331–351.

BARIDO-SOTTANI, J., VAN TIEL, N., HOPKINS, M. J., WRIGHT, D. F., STADLER, T. and WARNOCK, R. 2020. Ignoring fossil age uncertainty leads to inaccurate topology and divergence time estimates in time calibrated tree inference. *Frontiers in Ecology & Evolution*, **8**, 183.

BARRANDE, J. 1887. *Système Silurien du Centre de la Bohême. Vol. VII. Classe des Echinodermes, Ordre des Cystidées*. Rivnac, Praga, 233 pp.

BRUGUIÈRE, J. G. 1791. *Tableau Encyclopédique et Méthodique des Trois Règnes de la Nature, contenant l'Helminthologie, ou les Vers Infusoires, les Vers Intestins, les Vers Mollusques, etc*, **7**. Panckoucke, Paris.

ČERNÝ, D., MADZIA, D. and SLATER, G. J. 2022. Empirical and methodological challenges to the model-based inference of diversification rates in extinct clades. *Systematic Biology*, **71**, 153–171.

DRUMMOND, A. J., HO, S. Y. W., PHILLIPS, M. J. and RAMBAUT, A. 2006. Relaxed phylogenetics and dating with confidence. *PLoS Biology*, **4** (5), e88.

ELDREDGE, N. 1971. The allopatric model and phylogeny in Paleozoic invertebrates. *Evolution*, **25**, 156–167.

FATKA, O. and KORDULE, V. 2001. *Asturicystis havliceki* sp. nov. (Echinodermata, Homostelea) from the middle Cambrian of Bohemia (Barrandian area, Czech Republic). *Časopis České Geologické Společnosti (=Journal of the Czech Geological Society)*, **46**, 189–193.

FRIEDRICH, W. P. 1993. Systematik und Funktionsmorphologie mittelkambrischer Cincta (Carpoidea, Echinodermata). *Beringeria*, **7**, 3–190.

GAVRYUSHKINA, A., HEATH, T. A., KSEPKA, D. T., STADLER, T., WELCH, D. and DRUMMOND, A. J. 2017. Bayesian total-evidence dating reveals the recent crown radiation of penguins. *Systematic Biology*, **66**, 57–73.

HEATH, T. A., HEDTKE, S. M. and HILLIS, D. M. 2008. Taxon sampling and the accuracy of phylogenetic analyses. *Journal of Systematics & Evolution*, **46**, 239–257.

HEATH, T. A., HUELSENBECK, J. P. and STADLER, T. 2014. The fossilized birth–death process for coherent calibration of divergence-time estimates. *Proceedings of the National Academy of Sciences*, **111**, E2957–E2966.

HÖHNA, S., LANDIS, M. J., HEATH, T. A., BOUSSAU, B., LARTILLOT, N., MOORE, B. R., HUELSENBECK, J. P. and RONQUIST, F. 2016. RevBayes: Bayesian phylogenetic inference using graphical models and an interactive model-specification language. *Systematic Biology*, **65**, 726–736.

JAEKEL, O. 1918. Phylogenie und system der Pelmatozoen. *Paläontologische Zeitschrift*, **3**, 1–128.

KASS, R. E. and RAFTERY, A. E. 1995. Bayes factors. *Journal of the American Statistical Association*, **90**, 773–795.

KLEIN, J. T. 1734. *Naturalis dispositio echinodermatum. Accessit lucubratiuncula de aculeis echinorum marinorum, cum spicilegio de belemnitis*. Gedani, Schreiber, 79 pp.

LEWIS, P. O. 2001. A likelihood approach to estimating phylogeny from discrete morphological character data. *Systematic Biology*, **50**, 913–925.

MONGIARDINO KOCH, N., GARWOOD, R. J. and PARRY, L. A. 2021. Fossils improve phylogenetic analyses of morphological characters. *Proceedings of the Royal Society B*, **288** (1950), 20210044.

RAHMAN, I. A. and ZAMORA, S. 2009. The oldest cinctan carpoid (stem-group Echinodermata), and the evolution of the water vascular system. *Zoological Journal of the Linnean Society*, **157**, 420–432.

RAHMAN, I. A., ZAMORA, S., FALKINGHAM, P. L. and PHILLIPS, J. C. 2015. Cambrian cinctan echinoderms shed light on feeding in the ancestral deuterostome. *Proceedings of the Royal Society B*, **282**, 20151964.

RAHMAN, I. A., O'SHEA, J., LAUTENSCHLAGER, S. and ZAMORA, S. 2020. Potential evolutionary trade-off between feeding and stability in Cambrian cinctan echinoderms. *Palaeontology*, **63**, 689–701.

RAMBAUT, A., DRUMMOND, A. J., XIE, D., BAELE, G. and SUCHARD, M. A. 2018. Posterior summarization in Bayesian phylogenetics using Tracer 1.7. *Systematic Biology*, **67**, 901–904.

ROZHNOV, S. V. 2006. Carpozoan echinoderms from the middle Cambrian (Mayaktakh formation) of Siberia (lower reaches of the Lena river). *Paleontological Journal*, **40**, 266–275.

SDZUY, K. 1993. Early Cincta (Carpoidea) from the Middle Cambrian of Spain. *Beringeria*, **8**, 189–207.

SDZUY, K., LIÑÁN, E. and GOZALO, R. 1999. The Leonian Stage (early Middle Cambrian): a unit for Cambrian correlation in the Mediterranean subprovince. *Geological Magazine*, **136**, 39–48.

SMITH, A. B. and ZAMORA, S. 2009. Rooting phylogenies of problematic fossil taxa; a case study using cinctans (stem-group echinoderms). *Palaeontology*, **52**, 803–821.

SOUL, L. C. and FRIEDMAN, M. 2015. Taxonomy and phylogeny can yield comparable results in comparative paleontological analyses. *Systematic Biology*, **64**, 608–620.

SOUL, L. C. and WRIGHT, D. F. 2021. *Phylogenetic comparative methods: A user's guide for paleontologists*. Elements of Paleontology. Cambridge University Press.

STADLER, T. 2010. Sampling-through-time in birth–death trees. *Journal of Theoretical Biology*, **267**, 396–404.

STADLER, T., GAVRYUSHKINA, A., WARNOCK, R. C., DRUMMOND, A. J. and HEATH, T. A. 2018. The fossilized birth–death model for the analysis of stratigraphic range data under different speciation modes. *Journal of Theoretical Biology*, **447**, 41–55.

SWOFFORD, D. L. 2002. *Phylogenetic analysis using parsimony (and other methods). Version 4.0 Beta 10*. Sinauer Associates, Sunderland.

THUY, B., ERIKSSON, M. E., KUTSCHER, M., LINDGREN, J., NUMBERGER-THUY, L. D. and WRIGHT, D. F. 2022. Miniaturization during a Silurian environmental crisis generated the modern brittle star body plan. *Communications Biology*, **5** (1), 14.

UBAGHS, G. 1967. Homostelea. S565–S581. *In* MOORE, R. C. (ed.) *Treatise on invertebrate paleontology. Part S. Echinodermata 1*. The Geological Society of America & University of Kansas Press.

UBAGHS, G. 1975. Early Palaeozoic echinoderms. *Annual Review of Earth & Planetary Sciences*, **3**, 79–98.

WAGNER, P. J. 2000. The quality of the fossil record and the accuracy of phylogenetic inferences about sampling and diversity. *Systematic Biology*, **49**, 65–86.

WAGNER, P. J. 2012. Modelling rate distributions using character compatibility: implications for morphological evolution among fossil invertebrates. *Biology Letters*, **8**, 143–146.

WARNOCK, R. C. and WRIGHT, A. M. 2020. *Understanding the tripartite approach to Bayesian divergence time estimation* . Elements of Paleontology. Cambridge University Press.

WRIGHT, D. F. 2017. Bayesian estimation of fossil phylogenies and the evolution of early to middle Paleozoic crinoids (Echinodermata). *Journal of Paleontology*, **91**, 799–814.

WRIGHT, A. M. and HILLIS, D. M. 2014. Bayesian analysis using a simple likelihood model outperforms parsimony for estimation of phylogeny from discrete morphological data. *PLoS One*, **9** (10), e109210.

WRIGHT, A. M., WAGNER, P. J. and WRIGHT, D. F. 2021. *Testing character evolution models in phylogenetic paleobiology: a case study with Cambrian echinoderms*. Elements of Paleontology. Cambridge University Press.

XIE, W., LEWIS, P. O., FAN, Y., KUO, L. and CHEN, M. H. 2011. Improving marginal likelihood estimation for Bayesian phylogenetic model selection. *Systematic Biology*, **60**, 150–160.

ZAMORA, S. and ÁLVARO, J. J. 2010. Testing for a decline in diversity prior to extinction: Languedocian (latest mid-Cambrian) distribution of cinctans (Echinodermata) in the Iberian Chains, NE Spain. *Palaeontology*, **53**, 1349–1368.

ZAMORA, S. and SMITH, A. B. 2008. A new Middle Cambrian stem group echinoderm from Spain: palaeobiological implications of a highly asymmetric cinctan. *Acta Palaeontologica Polonica*, **53**, 207–220.

ZAMORA, S., LEFEBVRE, B., ÁLVARO, J. J., CLAUSEN, S., ELICKI, O., FATKA, O., JELL, P., KOUCHINSKY, A., LIN, J.-P., NARDIN, E., PARSLEY, R., ROZHNOV, S., SPRINKLE, J., SUMRALL, C. D., VIZCAÏNO, D. and SMITH, A. B. 2013*a*. Cambrian echinoderm diversity and palaeobiogeography. From: Harper, D. A. T. and Servais, T. (eds) 2013. Early Palaeozoic biogeography and palaeogeography. *Geological Society, London, Memoirs*, **38**, 157–171.

ZAMORA, S., RAHMAN, I. A. and SMITH, A. B. 2013*b*. The ontogeny of cinctans (stem-group echinodermata) as revealed by a new genus, *Graciacystis*, from the middle Cambrian of Spain. *Palaeontology*, **56**, 399–410.

APPENDIX

Character coding

Morphological character coding for *Bohemiacinctus havliceki* gen. nov. based on the phylogenetic character matrix in Zamora *et al.* (2013*b*).

01101 1??00 10100 00000 00222 02222 00100 120?0 10000 01222 10001 11210